Energy 138 (2017) 861–872

Contents lists available at ScienceDirect

Energy

journal homepage: www.elsevier.com/locate/energy

Economic dispatch of multiple energy carriers

Soheil Derafshi Beigvand [a], Hamdi Abdi [a,*], Massimo La Scala [b]

[a] Department of Electrical Engineering, Razi University, Kermanshah, Iran
[b] Electrical and Electronic Department (DEE) of the Polytechnic School of Bari (Politecnico di Bari), Bari, Italy

ARTICLE INFO

Article history:
Received 26 September 2016
Received in revised form
10 July 2017
Accepted 17 July 2017
Available online 18 July 2017

Keywords:
Energy hub
Gas loss formula
Hybrid system
Multiple energy carriers
Economic dispatch

ABSTRACT

Energy hubs can provide high flexibility in the operation of the integrated systems. This paper presents Time Varying Acceleration Coefficients Particle Swarm Optimization (TVAC-PSO) algorithm to optimize the Multiple Energy Carriers Economic Dispatch (MECED) problem for hybrid electrical and natural gas networks. The simulation results on two case studies are reported. The first one verifies an introduced gas loss formula and another one is devoted to a modified version of IEEE 14-bus test system. The results are compared with PSO, Genetic Algorithm (GA), and Differential Evolution (DE) technique. They show that a hybrid system can operate at a lower cost than independently-operated systems; CHP units can supply more electrical demand than the electrical network while their contribution in supplying the heat demand may be smaller than that of gas furnaces. In a hybrid system, energy efficiency can be reached, producing electrical power and heat locally; CHP units have a great role in reduction of operational cost; In the coupled mode, electrical power losses are decreased, while the gas losses are increased; The simple proposed gas loss formula can provide acceptable results; Cost reductions due to employing CHPs and applying the proposed optimization technique are greater than the other methods.

1. Introduction

The advent of new equipment for energy conversion and storage, dispersed generation, Combined Heat and Power (CHP) generation produced a general interest in a more efficient use of energy through exchanges of multiple energy carriers in urban smart districts, industrial parks, and large tertiary facilities involving the integration of distribution systems. At the same time, the need to make national energy infrastructures more resilient to global energy price volatility, supply and demand drastic changes due to new more affordable fuels such as the shale gas, new technologies coming up (renewables, poly-generation, etc.) or dramatic financial or geo-political crises renewed the interest toward the integration of multiple energy carriers at the transmission level [1].

Some examples of contact points between gas infrastructures and electricity ones are: large Combined Cycle Gas Turbine (CCGT) power plants, CHP generation for large industrial facilities, Liquefied Natural Gas (LNG) regasification terminal built close to gas infrastructures and power stations, Underground Natural Gas Storage (UNGS), Flex-Fuel Poly-generation (FFPG) conversion stations such as co-fired and dual-fueled plants [1,2], Integrated Gasification Combined Cycle (IGCC) technology and the so-called methane refineries capable to convert syngas into liquid hydrocarbons and electrical energy, etc. This new scenario opens the doors to a new coordinated way to plan national or regional energy infrastructures and introduce the concept of energy hubs, sometimes constituted by an entire region or nation, at the transmission level and long-distance transportation of energy [3]. Furthermore, more and more electrical energy is produced by renewables characterized by very different levelized production costs and a limited controlled capacity. Nowadays, renewable energy only relies on electrical transmission lines to be transferred from production to load centers, but new ways are available to convert Power to Gas (P2G) which creates a new connection between electrical and gas infrastructures [4,5].

Many evolved energy infrastructures have been developed during the second half of the 20th century, and it is questionable if they meet the today's (and also tomorrow's) power system

* Corresponding author. 67149-67346, Kermanshah, Iran.
E-mail address: hamdiabdi@razi.ac.ir (H. Abdi).

http://dx.doi.org/10.1016/j.energy.2017.07.108
0360-5442/

requirements. In addition to the congested transmission networks, a lot of facilities and infrastructures are approaching the end of their lifetime. Moreover, other challenges like the continuously growing different demands of energies, the power industries restructuring, the dependency on the finite fossil energy sources, and utilizing more environmentally friendly and sustainable energy resources raise the question of whether piecewise changes applied to the existing systems are sufficient to solve all these problems. Residential, commercial, and industrial consumers need different carriers provided by various energy infrastructures. In the industrialized world, petroleum products, coal, biomass, and the other carriers like natural gas, electricity, heat, and cool energies are typically utilized [6]. So far, different energy transportation infrastructures are planned and operated separately to meet reliability, efficiency, cost-effectiveness, and environmental requirements (e.g. for gas systems in Ref. [7] and for district heating systems in Ref. [8]). This leads to low efficiency and reliability, high operational cost and energy losses, etc. Because, for example, one type of loads like electricity can only be supplied by the power system and the other energy infrastructures do not have any role in supplying this demand (through converters).

Recently, an integrated view of energy networks in which various energy carriers such as electricity, natural gas, etc. are simultaneously optimized, has been suggested in Refs. [9–11] and different projects have been defined which can realize this viewpoint. For example [12], works on a type of converters to generate electricity. This can play a key role in the hubs where seawater is available. Another case can be found in Ref. [6] where a real energy hub is on the focus. In this context, the purpose of [13] is to develop and implement an energy hub management system.

Integration of multiple energy infrastructures on long distances and energy hubs increase the reliability from demand side; since different carriers can be locally converted into the desired form of energy and consequently various loads can be supplied by them. Conversely, the reliability of the individual infrastructures could be reduced (e.g. by reducing maintenance) while availability for the demand remains high [6]. It results in some difficulties to reinforce the existing grids in presence of permission delays, environmental concerns, geo-political instabilities, etc. The introduction of energy hubs and integration of long distance energy transportation grids allows for more flexibility in the operational optimization of networks and more efficiency since different forms of energy can be optimized depending on costs, availability, environmental impact, storage opportunities, etc.

Converter combinations in the form of energy hub provide the technology needed to integrate multiple energy carriers.

Natural gas and electricity Optimal Power Flow (OPF) have been presented in Ref. [14], in which the energy transformation between electrical and gas systems at the generators has been considered. Multiple Energy Carriers Optimal Power Dispatch (MECOPD) as a new concept in the optimization of energy hubs has been addressed in Ref. [15]. In fact, in Ref. [15], optimal dispatch problem has been introduced in the form of general optimization approach for power conversion and dispatch in the power networks containing several energy carriers such as electricity, natural gas, and district heating. In Ref. [16], a multi-objective optimization framework has been proposed for cost-environmental operation of a system of energy hubs in the presence of demand response program. Ref. [17], suggested the optimization of energy hub systems using a modified gravitational search algorithm based on self-adoptive learning strategy. Ref. [18] proposed a general stochastic optimization and modeling framework to solve scheduling problem of the wind integrated smart energy hub. A similar approach has been reported in Ref. [19]. OPF problem of multiple energy carriers including energy hubs has been proposed in Ref. [9]. A decomposed solution to this problem can be found in Ref. [11], in which the main problem has been decomposed into separate single energy carrier optimal power flow problems. Also, in Ref. [10] a modified teaching-learning based optimization technique has been introduced to optimize the energy flow through the multicarrier systems. In Refs. [20,21], an approach based on an improved version of gravitational search algorithm to solve Multiple Energy Carriers OPF (MECOPF) problem has been proposed. A mixed integer linear programming to calculate OPF in multicarrier energy systems has been introduced in Ref. [22].

Particle Swarm Optimization (PSO) is a population based optimization technique in which particles adjust their velocity and move in the solution space according to some simple rules to find optimum solutions. In addition to its simplicity, considering few assumptions about the under study problem is one of the major advantages of PSO over classic optimization approaches. Consequently, different difficult optimization problems associated with the power systems such as ED [23] and OPF [24] have been solved by PSO. Moreover, different versions of it (including combination with various methods) have been proposed and other energy system optimization problems have been solved. For example, in Ref. [25] a modified PSO has been suggested to find optimal solution of ED problem in power systems. Ref. [26] applied a differential evolution PSO to multi-area ED problems. The work presented in Ref. [27], combined PSO with an aging leader and challengers to solve OPF considering FACT devices. Ref. [28] formed a hybrid optimization algorithm using PSO to solve ED of CHPs where two carriers (i.e. electricity and heat) are involved.

In this paper, economic dispatch for multiple energy carriers and multiple hubs is proposed and solved by a powerful version of PSO technique, namely Time Varying Acceleration Coefficients PSO (TVAC-PSO). This is a first level of optimization based only on economical factors useful to represent integrated operations of multiple energy carriers. Some explicit gas and electricity loss formulas are introduced to simplify the formulation of the problem. This tool is a basic computational engine in studies for operational-planning and the evaluation of long-term investment strategies when high-capacity interregional energy transportation infrastructures have to be designed and analyzed in terms of technical and economic feasibility. The proposed approach consents to solve more energy hubs at the same time differently from MECOPD and introduce some modeling assumptions which avoid the whole representation of lines and pipelines as in MECOPF approach. The approximated loss formulas for transmission losses and pipeline losses allow a simple representation and an efficient software structure which makes the approach prone for operational planning purposes and numerous simulations needed for technical-economic analyses in long-term planning.

1.1. Contributions

1) Gas Loss Formulation

It is first time that an explicit gas loss formula is proposed for the optimization purpose. The suggested formulation is simple and shows a linear relationship between gas losses in the pipeline networks and the produced gas by gas stations.

2) Multiple Energy Carriers Economic Dispatch

In this paper, an ED problem of multiple energy carriers with respect to electric-gas networks is proposed focusing on long-distance energy transportation. In fact, the main contribution of our work is the introduction of a novel model, called Multiple Energy Carriers Economic Dispatch (MECED) problem for transmission network. The rationale is to provide a computationally efficient tool for dispatching electricity and gas on an economical basis taking into account gas and electricity losses for long-distance energy transportation systems. The procedure can find applications whenever it is possible to switch from an energy carrier to another to supply energy demands. The same approach can also be applied for short-term analysis considering that, although gas price is always fixed on this time horizon because of take-or-pay contracts, electricity may quickly change price on the spot-market and perhaps it may result more convenient to switch to different fuels, to increase CHP production, take advantage of gas stored in UNGS or LNG regasifiers, etc.

3) Applying an Optimization Algorithm to MECED

TVAC-PSO as an improved version of PSO is used to solve the proposed optimization problem. This algorithm has been successfully applied to various nonlinear problems and results demonstrated its high performance in terms of providing a good quality solution and fast convergence speed [29,30]. In this work, a new algorithm based on the TVAC-PSO is proposed. The main contribution in this area derives from the capability of the algorithm in being robust, i.e. capable of finding an optimum solution without convergence problems and mostly yielding a better optimum with regard to other tested algorithms (such as PSO, Genetic Algorithm (GA), and Differential Evolution (DE)) which results in economical benefits.

It should be noted that, in this paper, “energy” and “pipeline network” are used to refer to “electrical or gas” and “gas-based system,” respectively. Also, the use of the term “multiple energy carriers” in our paper, is referred as a synonym of term “hybrid” [31,32].

2. Basic concepts and assumptions

The formulation of ED (for both real and reactive powers) is well known for electrical systems (distribution and transmission grids) and has been discussed in many publications [33,34]. Differently, in the multiple energy systems, it should be re-formulated and adapted to new needs. In this paper, MECED problem for transmission network is formulated using a different method. It is important to note that, we mainly focus on electrical and gas

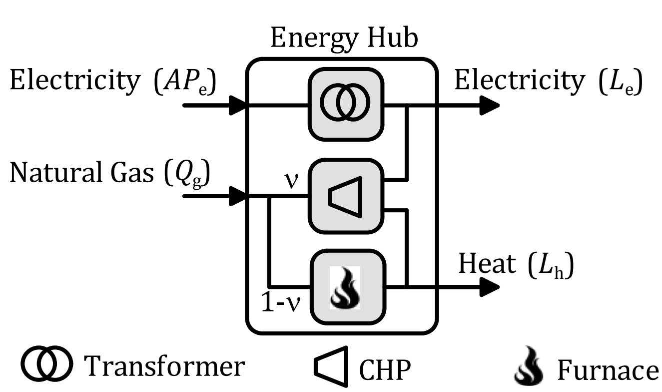

Fig. 1. A special case of energy hub [9]. Note: Transformer consumes and provides electricity at its input (AP_e) and output (a fraction of L_e), respectively. CHP unit produces electricity (the rest of L_e) and heat (a fraction of L_h) through consuming the natural gas (equal to $\nu \times Q_g$). A gas furnace burns the natural gas (equal to $(1-\nu) \times Q_g$) and delivers heat (the rest of L_h).

networks as in Refs. [9,31,35] to show how the ED problem can be derived. In our developments, without lack of generality, active power loss is considered in problem formulation.

This is a first formulation of the problem to assess the feasibility of the approach and algorithmic features of the proposed method. Without losing generality, other carriers can be similarly treated.

In general, an energy hub establishes an interface between delivered energy (by transmission networks and/or energy sources) and loads. The basic hub elements can be found in Refs. [1,2,9]. Fig. 1 shows a special energy hub containing transformer, CHP, and a gas furnace as the convertor elements which consume electricity and natural gas to supply the electrical and heat demands.

In this paper, the following assumptions are used for constructing each problem element: 1) The system is considered in steady-state conditions and only affected by steady-state losses. 2) Energy flow through each convertor is only characterized through its constant efficiency [9]. 3) Within each energy hub, losses only occur in the convertor devices. 4) Storage devices according to [9,36] can be included. But, in this paper, they are not considered. 5) It is assumed that there is no pipeline leakage. 6) As commonly practiced for electricity and natural gas, the cost of the energy carriers is stated as the polynomial functions of the corresponding energy [9,14,15,37]. 7) For obtaining the gas loss formula, a constant compression ratio for each compressor is assumed.

3. Problem formulation

3.1. Electrical power losses

Line losses should be taken into account to meet the load demand completely. It is well known that the total system loss is a function of electrical power generation of all the generators. One of the most popular approaches for calculating the total power losses without using power flow equations explicitly, is Kron's loss formula which is known as *B*-matrix method. This loss formulation simplifies the calculations since the system transmission losses can be directly evaluated as follows [37]:

$$AP_{\text{loss}} = \sum_{i=1}^{N_{eg}} \sum_{j=1}^{N_{eg}} AP_i^g Bl_{ij} AP_j^g + \sum_{i=1}^{N_{eg}} Bl_{0i} AP_i^g + Bl_{00} \tag{1}$$

where AP_{loss} and $AP^g a$ are the active power loss and active power production, respectively; coefficients Bl_{ij}, Bl_{0i}, and Bl_{00} with $i,j = 1,\ldots,N_{eg}$ denote the *B*-coefficients which are assumed to be constant; N_{eg} represents the number of all generation units.

A straightforward approach for calculating the *B*-coefficients has been addressed in Ref. [37]. Note that, the other formulations could be easily employed to evaluate AP_{loss} in other types of electrical systems. Finally, the following equation has to be satisfied.

$$\text{Production} = \text{Demand} + \text{Losses} \tag{2}$$

3.2. Gas losses

Similar to the electrical system, energy flow analysis of a pipeline network can be described by stating the nodal energy balance and line equations. The following equation represents the flow balance for the i^{th} node [9]:

$$Q_i = \sum_{j \in N_i} Q_{ij} \tag{3}$$

where Q_i denotes the volume flow injected at the i^{th} node; N_i is the

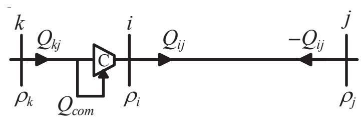

Fig. 2. Model of a pipeline equipped with compressor (C) [9].

set of nodes connected to the i^{th} node; Q_{ij} denotes the pipeline flow which can be expressed as follows:

$$Q_{ij} = k_{ij}s_{ij}\sqrt{\left|\rho_i^2 - \rho_j^2\right|} \text{ with } s_{ij} = \begin{cases} +1, & \text{if } \rho_i \geq \rho_j \\ -1, & \text{if otherwise} \end{cases} \quad (4)$$

and where ρ_i and ρ_j are the upstream and downstream pressures, respectively, as shown in Fig. 2; k_{ij} represents the properties of the pipeline and fluid (for more details, see Ref. [9]).

Fig. 2 shows a pipeline equipped with a compressor. The energy consumption of a compressor (i.e. Q_{com}) can be expressed as a function of the pressure difference between the output and input of the compressor (i.e. $(\rho_i - \rho_k)$), multiplied by a constant characterizing the compressor unit (i.e. k_{com}) and the volume flow rate through it (i.e. Q_{ij}) [9] as follows:

$$Q_{com} = k_{com}Q_{ij}(\rho_i - \rho_k) \quad (5)$$

Also, the compression ratio ρ_{cr} of the mentioned compressor can be defined as follows:

$$\rho_{\text{cr}} = \rho_i/\rho_k \quad (6)$$

Consequently

$$Q_{kj} = Q_{ij} + Q_{com} \quad (7)$$

For more information about energy flow computation in the natural gas networks, see Refs. [38–40]. It is clear that, in a pipeline equipped with a compressor unit as shown in Fig. 2, natural gas flows from node k to node j since the compression ratio is a positive number [9,35] (see Section 6). In this context, Q_{kj} can be considered as a net gas injection into bus k.

It is essential to note that, in this paper, energy flows in the gas networks are described by conservation laws such as (3) or (7) and physical losses are usually not considered in equations [9,35]. Thus, for deriving the gas loss formula, the compressor demands are considered as the gas losses in the pipeline network. Therefore, a pipeline network without any compressor unit represents a lossless system. General flow equation presented in (4) allows to consider a wide range of transferable energy such as liquid and gaseous carriers [9]. In other words, our proposed approach is general enough to consider different fuels in order to obtain loss formula including various device representations. Thus:

$$Q_{\text{loss}} = \sum_{n=1}^{N_{com}} Q_{com_n} \quad (8)$$

where Q_{loss} denotes the gas losses and N_{com} is the total number of compressor units.

Q_{com_n} in (8) can be calculated for a specified operating condition. Thus, Δ can represent the small deviation from this point and we can write:

$$Q'_{com_n} = Q_{com_n} + \Delta Q_{com_n} \quad (9)$$

where Q'_{com_n} represents the new gas losses (compressors demands) for ΔQ_{com_n}.

Based on (9), Q_{loss} for a new operating point (i.e. Q'_{loss}) can be written as follows:

$$Q'_{\text{loss}} = \sum_{n=1}^{N_{com}} Q'_{com_n} = Q_{\text{loss}} + \sum_{n=1}^{N_{com}} \Delta Q_{com_n} \quad (10)$$

For small changes, we can write:

$$\Delta Q_{com_n} = \frac{\partial Q_{com_n}}{\partial Q_{N_m}} \Delta Q_{N_m} \quad (11)$$

where Q_{N_m} denotes the supplied gas by the m^{th} adjacent network (gas source).

In general, $\frac{\partial Q_{com_n}}{\partial Q_{N_m}}$ for each compressor unit can be determined for a specific operating point based on the chain rule. An important assumption for obtaining the gas loss formula is to assume a constant compression ratio for each compressor. The gas loss formula can be obtained in the following manner:

Step 1. Calculate Q_{loss} for a specific operating point.
Step 2. Determine $\frac{\partial Q_{com_n}}{\partial Q_{N_m}}$ for each compressor unit.
Step 3. State ΔQ_{com_n} using (11).
Step 4. Formulate Q'_{loss} using (10).

It should be noted that, if several compressors are supplied through a single bus, a dispatch factor *df* assumed to be constant (similar to the energy hubs) can be considered to enhance accuracy.

3.3. Simple modeling of several energy hubs

A general model covering couplings with multiple inputs and outputs can be found in Ref. [9]. In this paper, we mainly focus on the energy hub presented in Fig. 1. Hence, according to [9], we can write:

$$L_{e_i} = \eta_{T_i} AP_{e_i} + \nu_i \eta_{GT_{e_i}} Q_{g_i} \quad (12)$$

$$L_{h_i} = \left[\nu_i \eta_{GT_{h_i}} + (1 - \nu_i)\eta_{F_i}\right] Q_{g_i} \quad (13)$$

with $i = 1, 2, \ldots, N_{hub}$ where AP_{e_i} and Q_{g_i} are the electricity (active load demand) and natural gas as inputs of the i^{th} hub; L_{e_i} and L_{h_i} denote electricity (active power) and heat as outputs; η_{T_i}, η_{F_i}, $\eta_{GT_{e_i}}$, and $\eta_{GT_{h_i}}$ represent the efficiencies of transformer (electricity-electricity), gas furnace (gas-heat), CHP (gas-electricity), and CHP (gas-heat) of the i^{th} hub, respectively; ν_i is the dispatch factor of the i^{th} hub.

For a system containing N_{hub} energy hubs, on the basis of (12) and (13), total electricity (i.e. $L_{e_{\text{total}}}$) and heat (i.e. $L_{h_{\text{total}}}$) demands can be written as follows:

$$L_{e_{\text{total}}} = \sum_{i=1}^{N_{hub}} L_{e_i} + \sum_{i \in OED} AP_{ed_i} \quad (14)$$

$$L_{h_{\text{total}}} = \sum_{i=1}^{N_{hub}} L_{h_i} \quad (15)$$

where *OED* denotes the set of Other Electrical Demands directly connected to the electrical network.

Note that, heat demands can be supplied through energy hubs only. Also, for more flexibility, in this paper, we consider ν as a variable depending on the operating conditions. Finally, a compact

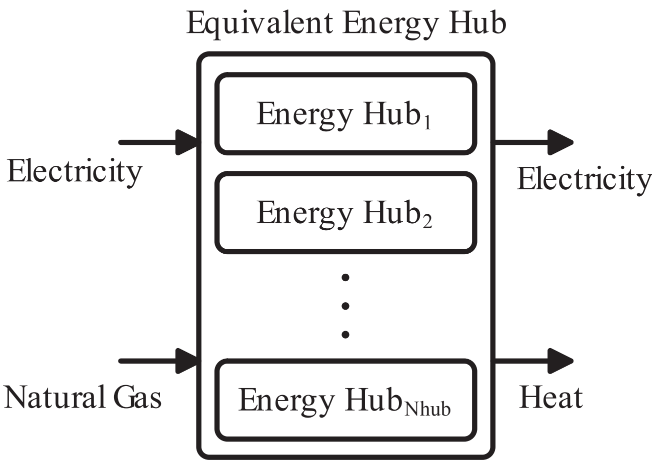

Fig. 3. A compact form of several energy hubs.

form of several energy hubs can be regarded as shown in Fig. 3.

3.4. Economic dispatch problem of multiple energy carriers

The MECED problem is stated as follows: Minimize

$$OF = \sum_{i=1}^{N_{eg}} \left[ae_i + be_i AP_i^g + ce_i \left(AP_i^g \right)^2 \right] + \sum_{i=1}^{N_{an}} \left[ag_i + bg_i Q_{N_i} + cg_i \left(Q_{N_i} \right)^2 \right] \quad (16)$$

subject to

$$\sum_{i=1}^{N_{eg}} AP_i^g - AP_{loss} - \sum_{i=1}^{N_{hub}} \frac{L_{e_i} - \frac{\nu_i \eta_{GT_{e_i}}}{\nu_i \eta_{GT_{h_i}} + (1-\nu_i)\eta_{F_i}} L_{h_i}}{\eta_{T_i}} - \sum_{i \in OED} AP_{ed_i} = 0 \quad (17)$$

$$\sum_{i=1}^{N_{an}} Q_{N_i} - Q'_{loss} - \sum_{i=1}^{N_{hub}} \frac{L_{h_i}}{\nu_i \eta_{GT_{h_i}} + (1-\nu_i)\eta_{F_i}} = 0 \quad (18)$$

$$AP_{i,\min}^g \le AP_i^g \le AP_{i,\max}^g, i = 1, 2, \ldots, N_{eg} \quad (19)$$

$$0 \le \nu_i \le 1, i = 1, 2, \ldots, N_{hub} \quad (20)$$

where OF denotes the objective function in which the total energy cost including active power generation cost and gas power production cost is selected [9]; ae, be, ce, ag, bg, and cg are the cost coefficients; also, subscripts min and max represent the minimum and maximum values of a quantity; and N_{an} denotes the number of adjacent networks (gas sources).

Note that, (17) and (18) represent the balance equations (considering (12) and (13)) related to the electrical and gas systems, respectively. In fact, the energy balance Equation (2) for other energy networks can be added to the equality constraints. Moreover, it should be mentioned that active power generations, gas power productions, and dispatch factors of hubs are independent (control) variables and the other variables are dependent (state) ones.

4. TVAC-PSO structure

PSO was proposed by Kennedy and Eberhart in 1995 [41]. This algorithm is based on the simulation of social behavior such as flock of birds and can optimize a function by conducting a population-based stochastic search. The population of particles is updated by applying an operator according to the fitness information. This information is based on the environment such that the individuals of the population can be expected to approach the better position.

In the TVAC-PSO algorithm, the updated velocity and position of each particle at $(t+1)^{\text{th}}$ iteration can be determined as follows [29]:

$$\pi_i^d(t+1) = w(t)\pi_i^d(t) + CC_1 \text{rand}_1 \left(pbest_i^d - x_i^d(t) \right) + CC_2 \text{rand}_2 \left(gbest^d - x_i^d(t) \right) \quad (21)$$

$$x_i^d(t+1) = x_i^d(t) + CC_0 \pi_i^d(t+1) \quad (22)$$

where $X_i = (x_i^1, \ldots, x_i^d, \ldots, x_i^n)$ and $Ve_i = (\pi_i^1, \ldots, \pi_i^d, \ldots, \pi_i^n)$ denote the position and velocity of the i^{th} particle such that x_i^d and π_i^d represent the position and velocity of the i^{th} particle in the d^{th} dimension; $pbest_i = (pbest_i^1, \ldots, pbest_i^d, \ldots, pbest_i^n)$ and $gbest = (gbest^1, \ldots, gbest^d, \ldots, gbest^n)$ are the best previous position of the i^{th} particle and the best previous position among all particles in the population, respectively; rand_1 and rand_2 denote two random numbers in the interval [0, 1]; CC_0 represents the constriction factor and can be determined as follows [29,42]:

$$CC_0 = \frac{2}{\left| 2 - \vartheta - \sqrt{\left| \vartheta^2 - 4\vartheta \right|} \right|} \quad (23)$$

where $\vartheta = CC_1 + CC_2$; the inertia weight $w(t)$ can be calculated as follows:

$$w(t) = w_{\text{initial}} - \frac{w_{\text{initial}} - w_{\text{final}}}{\text{Iteration}_{\max}} \times t \quad (24)$$

where w_{initial} and w_{final} denote the initial and final weights, respectively; also, $\text{Iteration}_{\max}$ represents the maximum number of iterations; and finally, CC_1 and CC_2 are cognitive and social component acceleration factors, respectively, which should be updated as follows [29,30,41]:

$$CC_1 = CC_{1,\text{initial}} + \frac{CC_{1,\text{final}} - CC_{1,\text{initial}}}{Iteration_{\max}} \times t \quad (25)$$

$$CC_2 = CC_{2,\text{initial}} + \frac{CC_{2,\text{final}} - CC_{2,\text{initial}}}{Iteration_{\max}} \times t \quad (26)$$

where $\{CC_{1,\text{initial}}, CC_{1,\text{final}}\}$ and $\{CC_{2,\text{initial}}, CC_{2,\text{final}}\}$ represent the initial and final values of cognitive and social component acceleration coefficients, respectively.

Note that, in order to improve the quality solution, TVAC-PSO selects the optimal values for CC_1 and CC_2. In comparison with the classical PSO, TVAC-PSO changes CC_1 and CC_2 linearly, while, classical PSO adopts two constant values for them. Variable values are because of the fact that, a relatively bigger value of CC_2 compared with CC_1 (i.e. $CC_2 > CC_1$) leads particles to a local optimum prematurely and relatively high values of CC_1 (i.e. $CC_1 > CC_2$) results to wander the particles around the search space [29,30,41]. So, in each iteration, CC_1 should be reduced and CC_2 should be increased. These can be realized by choosing appropriate values for $\{CC_{1,\text{initial}}, CC_{1,\text{final}}\}$ and $\{CC_{2,\text{initial}}, CC_{2,\text{final}}\}$.

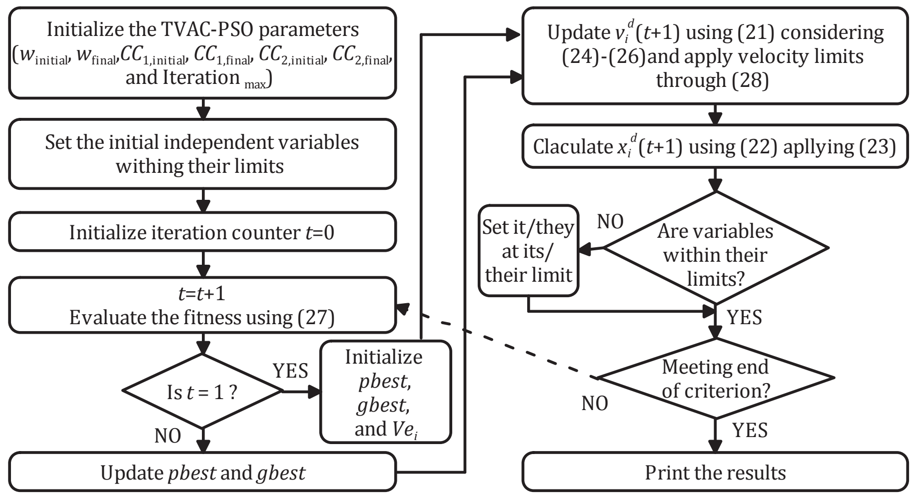

Fig. 4. Flowchart of TVAC-PSO-based MECED problem.

5. TVAC-PSO algorithm for MECED

The proposed TVAC-PSO-based MECED algorithm is illustrated in Fig. 4 and its different steps are presented below.

Step 1 (Initialization). Initialize the parameters of TVAC-PSO such as w_{initial}, w_{final}, $CC_{1,\text{initial}}$, $CC_{1,\text{final}}$, $CC_{2,\text{initial}}$, $CC_{2,\text{final}}$, and $\text{Iteration}_{\max}$ and then create random feasible initial population. Also, set the initial iteration $t = 0$.

Step 2 (Fitness evaluation). Firstly, set $t = t + 1$. Then, calculate the value of fitness for all particles. In this work, the penalty method has been selected as below to meet all equality constraints:

$$\begin{aligned}\text{fitness} &= \text{OF} \\ &+\text{Penalty}_1\left(\sum_{i=1}^{N_{eg}} AP_i^g - AP_{\text{loss}} - \sum_{i=1}^{N_{hub}} \frac{L_{e_i} - \frac{v_i \eta_{GTe_i}}{v_i \eta_{GTh_i} + (1-v_i)\eta_{F_i}} L_{h_i}}{\eta_{T_i}} - \sum_{i \in OED} AP_{ed_i}\right)^2 \\ &+\text{Penalty}_2\left(\sum_{i=1}^{N_{an}} Q_{N_i} - Q'_{\text{loss}} - \sum_{i=1}^{N_{hub}} \frac{L_{h_i}}{v_i \eta_{GT_{h_i}} + (1-v_i)\eta_{F_i}}\right)^2\end{aligned} \tag{27}$$

where Penalty_1 and Penalty_2 are the weighting factors (penalty parameters). Note that, in the above formula, in order to achieve a feasible solution, the weighting factors of both penalty functions are increased along the iterative process.

Step 3 (pbest and gbest initialization/update). If $t = 1$, then, the calculated fitness values in the Step 2 for the initial particles are considered as the initial values of *pbest*. The best value among all them is considered as *gbest*; else, update *pbest* and *gbest*.

Step 4 (Velocity update and evaluation). Update the velocity using (21) applying (24)–(26). Note that, in this step, the maximum velocity for the d^{th} dimension is considered as follows:

$$\pi_{\max}^d = \frac{x_{\max}^d - x_{\min}^d}{R} \tag{28}$$

where R is randomly chosen between $R_{\min}$ and $R_{\max}$ to control the number of intervals in the d^{th} dimension. So, the particle velocities should be in the range $[-\pi_{\max}^d, \pi_{\max}^d]$. The maximum velocity is set to 10–20% of the dynamic range of variable on each dimension.

Step 5 (Position update and evaluation). Update the position of particles through (22). Then, check that all variables are within their limits. If any of them violates or hits the limit, set it at its limit value (upper or lower).

Step 6 (Stopping criterion). If the age of algorithm (i.e. iteration) is equal or less than the maximum iteration (i.e. $t \le \text{Iteration}_{\max}$), then go to Step 2. Otherwise, go to Step 7.

Step 7. Print the results.

6. Case study simulations and results

The purpose of this section is to describe the suggested MECED problem and gas loss formula. So, these approaches are illustrated

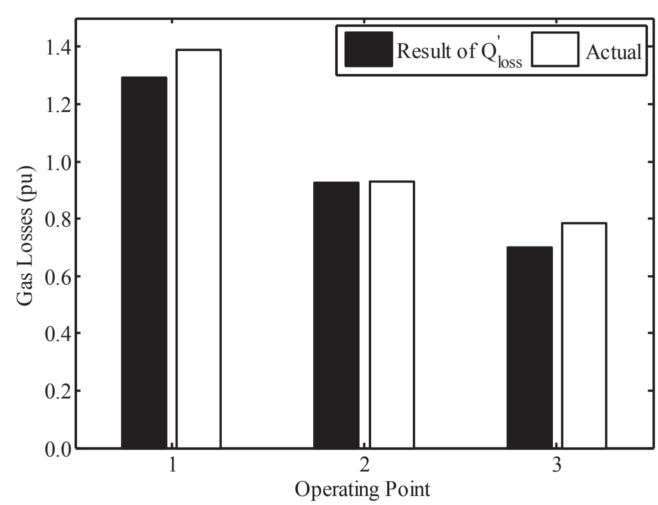

Fig. 5. Gas losses of the network under different operating conditions. Note: $L_{e_{\text{total}}} = 3.4131$ pu and $L_{h_{\text{total}}} = 6.5$ pu for first operating point, $L_{e_{\text{total}}} = 3.0152$ pu and $L_{h_{\text{total}}} = 6.0$ pu for second operating point, and $L_{e_{\text{total}}} = 2.7960$ pu and $L_{h_{\text{total}}} = 5.3$ pu for third operating point.

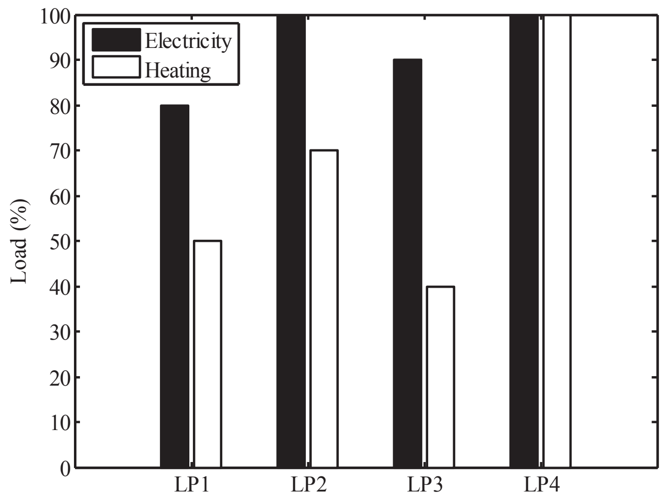

Fig. 6. Different load profiles investigated for test case B.

using two case studies (simple and complex ones). In fact, the first test case is selected to verify the proposed gas loss formula and, thus, we mainly focus on it in Subsection 6.1. The second test case is proposed to illustrate the suggested problem on a more complex network. It should be mentioned that, in these examples, underlined numbers denote the gas node, while normal numbers imply the electrical buses.

The proposed approach has been programmed in MATLAB environment and implemented on an Intel Pentium CPU 2.0 GHz with 2GB RAM, PC, in which it has been run more than 50 times. Also, for the second test case, the results of TVAC-PSO-based MECED problem in terms of quality solution and convergence speed have been compared with various well-known and programmed algorithms such as GA, PSO, and DE to show the ability of the introduced algorithm in finding an operating point with lower objective function. So, parameters of the TVAC-PSO are fixed as follows: $w_{\text{initial}} = 0.9$, $w_{\text{final}} = 0.4$, $CC_{1,\text{final}} = CC_{2,\text{initial}} = 0.5$, $CC_{1,\text{initial}} = CC_{2,\text{final}} = 2.5$, $R_{\min} = 5$, $R_{\max} = 10$, $\text{Iteration}_{\max} = 100$, and the population size is 100.

Table 2
Simulation results of test case B using TVAC-PSO, PSO, GA, and DE Techniques – without CHP units (conventional operation).

LP No.	Technique	Gas Production[a]			Power Generation[a]		OF[b]
		Q_{N_1}	Q_{N_2}	Q_{N_3}	AP_1^g	AP_2^g	
1	TVAC-PSO	1.6679	3.5284	0.0103	0.4823	1.6482	26.3051
	PSO	2.6435	2.8250	0.0000	0.0000	2.1301	26.4021
	GA	6.5235	0.0000	0.0000	0.9039	1.2361	27.5599
	DE	0.0000	0.0000	7.0468	2.2244	0.0000	28.6966
2	TVAC-PSO	2.3850	3.8651	1.3282	0.5058	2.1748	33.9376
	PSO	1.8041	2.7740	3.5745	1.2318	1.4689	34.2970
	GA	0.0000	2.8706	5.3801	0.8445	1.8424	34.6028
	DE	2.4347	0.0000	7.0089	0.3585	2.3212	35.4049
3	TVAC-PSO	1.4171	2.8444	0.0000	0.4598	1.9443	28.0367
	PSO	0.0000	3.8762	0.0000	0.0000	2.4049	28.1650
	GA	5.3237	0.0000	0.0000	0.8317	1.5795	28.9429
	DE	0.0000	0.0000	5.7507	2.5000	0.0234	30.3017
4	TVAC-PSO	3.4065	4.1680	3.6638	0.5141	2.1666	37.3629
	PSO	3.4301	3.2327	5.0258	0.6877	1.9956	37.6003
	GA	0.2130	5.9771	4.4293	0.8833	1.8046	37.7211
	DE	0.0000	9.1179	0.0000	0.4571	2.2231	38.3128

Note #1: [mu] denotes monetary unit.
Note #2: in this case, all dispatch factors are equal to 0.
[a] In [pu].
[b] In [mu].

6.1. Test case A

The aim of this example is to show the effectiveness of the proposed gas loss formula. Network data and the system condition are adopted from Ref. [9]. Under this condition, $Q_{\text{loss}} = 1.0767$ pu. Based on the suggested approach for calculating the gas loss formula, we have:

$$Q'_{\text{loss}} = \underbrace{1.0767}_{Q_{loss}} + \underbrace{(0.0377)}_{df_1 \frac{\partial Q_{com_1}}{\partial Q_N}} \Delta Q_N + \underbrace{(0.0344)}_{df_2 \frac{\partial Q_{com_2}}{\partial Q_N}} \Delta Q_N \tag{29}$$

Three arbitrary operating points are considered to evaluate the accuracy of the obtained gas loss formula as shown in Fig. 5. The first and third points show the ones far from the current

Table 1
Simulation results of test case B using TVAC-PSO, PSO, GA, and DE techniques – with CHP units.

LP No.	Technique	Operating Point													OF[b]
		Gas Production[a]			Power Generation[a]		Dispatch Factor								
		Q_{N_1}	Q_{N_2}	Q_{N_3}	AP_1^g	AP_2^g	ν_1	ν_2	ν_3	ν_4	ν_5	ν_6	ν_7	ν_8	
1	TVAC-PSO	1.7688	4.1354	1.5051	0.6133	0.3604	0.2160	0.5070	0.2817	0.9785	0.9978	1.0000	0.1335	0.4439	16.7735
	PSO	1.7207	4.1056	1.5375	0.6302	0.3730	0.1954	0.5081	0.2589	0.9586	0.9943	1.0000	0.1086	0.4342	17.0171
	GA	1.7263	3.9492	1.5690	0.6164	0.4753	0.2028	0.5127	0.1534	0.8877	0.9417	0.9935	0.1288	0.4083	17.7441
	DE	2.3788	2.7487	2.4948	0.5820	0.5776	0.2100	0.2240	0.1651	1.0000	0.9862	1.0000	0.1450	0.0602	18.4176
2	TVAC-PSO	3.7360	2.3515	5.5408	0.6655	0.4184	0.1977	0.4716	0.2571	0.9923	1.0000	1.0000	0.1304	0.4054	21.4203
	PSO	3.7776	2.2723	5.5335	0.6891	0.4320	0.1924	0.4448	0.2260	0.9848	0.9966	1.0000	0.1240	0.3991	21.7377
	GA	3.5520	2.8249	4.8357	0.6633	0.5127	0.1294	0.4687	0.1999	0.9914	1.0000	0.9999	0.1171	0.2793	21.9760
	DE	2.3282	5.2382	2.2731	0.6773	0.6387	0.1288	0.0000	0.2542	0.9903	1.0000	1.0000	0.0000	0.3544	22.7649
3	TVAC-PSO	1.0219	3.6006	1.5972	0.2792	1.0519	0.2957	0.6593	0.3788	1.0000	1.0000	1.0000	0.1984	0.5758	19.1861
	PSO	0.9630	3.5444	1.5921	1.2679	0.1639	0.2069	0.6571	0.2998	0.9992	0.9996	0.9994	0.0897	0.5294	19.9829
	GA	0.8287	3.4560	1.6857	0.7837	0.7117	0.2491	0.6517	0.0000	0.9976	1.0000	1.0000	0.1789	0.3217	20.5282
	DE	2.7750	1.4126	2.4240	1.0729	0.5213	0.1629	0.2531	0.0000	1.0000	1.0000	1.0000	0.0983	0.5033	21.5952
4	TVAC-PSO	4.1598	5.4269	5.1647	0.3314	0.4013	0.1423	0.3534	0.1867	0.8067	1.0000	1.0000	0.0930	0.3008	21.7043
	PSO	5.8449	4.1878	5.1810	0.3286	0.4050	0.1423	0.3532	0.1862	0.8066	0.9998	1.0000	0.0930	0.3005	21.9239
	GA	5.9964	4.0172	5.1848	0.6788	0.1008	0.1421	0.3517	0.1865	0.8050	0.9999	1.0000	0.0000	0.2975	22.3141
	DE	5.4569	4.1190	5.5000	0.4614	0.3664	0.1409	0.3531	0.1851	0.8059	0.9790	0.9745	0.0866	0.2053	22.6646

Note: [mu] denotes monetary unit.
[a] In [pu].
[b] In [mu].

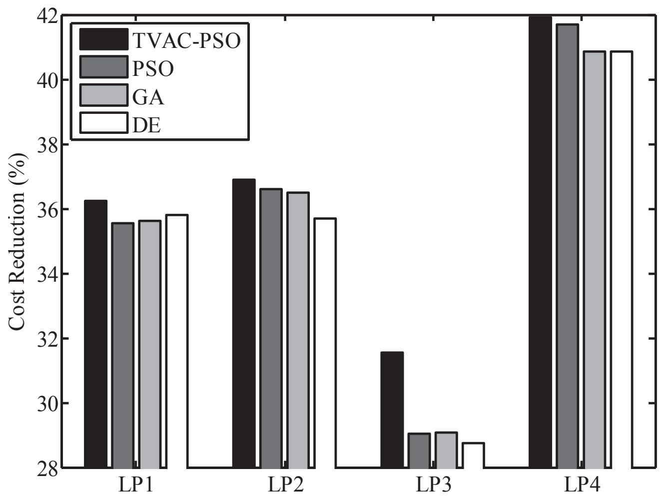

Fig. 7. Cost reduction in percentage due to the presence of CHP units.

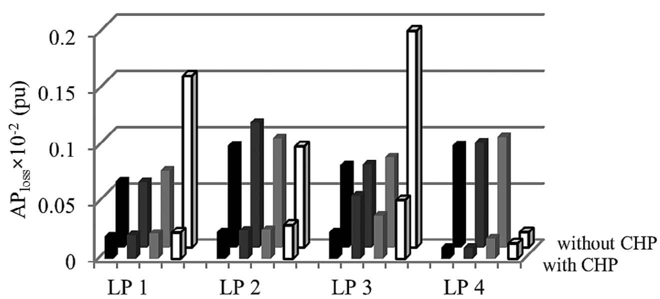

Fig. 8. Electrical power losses. Note: black, grey, dim-grey and white colors denote TVAC-PSO, PSO, GA, and DE, respectively.

operating point, while the second point illustrates a point close to the current one, but with a different loading. This figure indicates that the proposed formula for calculating the gas losses offers an acceptable solution. Absolute errors for the first, second, and third operating points are 6.98%, 0.59%, and 11.18%, respectively. In fact, it shows the main advantage of the linearized gas loss formula when strong nonlinearities of real gas losses are expected. It should be noted that the larger absolute error (i.e. 11.18%) is mainly due to the following assumptions: 1) The compression ratio remains constant (i.e. $\rho_{cr} = \text{constant}$). This assumption is valid as long as all bus pressures do not meet their limitations. In this condition, the compression ratio will be fixed to a minimum value (i.e. $\rho_{cr} = 1.2$). Hence, in order to fix the bus pressure to its limits (mainly, minimum value which is equal to 0.8 pu) when a bus pressure is violated, compression ratio must be increased. Thus, it can increase the absolute error. 2) There are two compressors which are fed from bus $\underline{1}$ (see Ref. [9]). So, as previously mentioned, for calculating the gas loss formula, we assume that $df = \text{constant}$. It is clear that this factor changes by changing the operating point. Thus, it can increase the absolute error.

6.2. Test case B

A new complex test case proposed in Ref. [20] is selected to evaluate the performance of the proposed economic dispatch problem. The system data can be found in Appendix.

Total active electricity demand and heat load are 2.590 and 6.750 pu, respectively. For current operating point as the basic condition, by using the method presented in Ref. [37], electrical loss formula is obtained as follows:

$$AP_{\text{loss}} = \begin{bmatrix} AP_1^g & AP_2^g \end{bmatrix} \underbrace{\begin{bmatrix} 0.0292 & 0.0096 \\ 0.0096 & 0.0128 \end{bmatrix}}_{Bl} \begin{bmatrix} AP_1^g \\ AP_2^g \end{bmatrix} + \underbrace{\begin{bmatrix} 0.0031 & -0.0005 \end{bmatrix}}_{Bl_0} \begin{bmatrix} AP_1^g \\ AP_2^g \end{bmatrix} + \underbrace{0.0011}_{Bl_{00}} \quad (30)$$

Also, the gas loss formula will be obtained as follows:

$$Q'_{\text{loss}} = \underbrace{3.4541}_{Q_{\text{loss}}} + \underbrace{(0.2499)}_{\frac{\partial Qcom_1}{\partial Q_{N_1}}} \Delta Q_{N_1} + \underbrace{(-0.0302)}_{\frac{\partial Qcom_2}{\partial Q_{N_2}}} \Delta Q_{N_2} + \underbrace{(0.3056)}_{\frac{\partial Qcom_3}{\partial Q_{N_3}}} \Delta Q_{N_3} \quad (31)$$

The proposed economic problem through (16)–(20) is implemented on the mentioned hybrid system for four different Load Profiles (LPs) presented in Fig. 6. For these profiles, the base electrical (active power) and heat demands are 2.590 and 6.750 pu, respectively. Also, note that, different investigations may be carried out using the presented economic dispatch method. In this test case, the system performance in terms of utilization of the CHP units within the hubs is focused on.

The optimization results obtained by TVAC-PSO, PSO, GA, and DE are illustrated in Table 1 where CHP are included in simulations and in Table 2 where no CHP unit is considered. Note that, in the case of conventional operation, all dispatch factors are set to 0; because CHP units should not be considered in the optimization problem. It can be observed from these tables that the proposed TVAC-PSO technique reaches a better solution for all LPs if compared with other techniques such as PSO, GA, and DE algorithms. From Tables 1 and 2, it can be seen that optimally utilization of CHP units can significantly reduce the production cost. From this view point, Fig. 7 shows different reductions in the generation costs for various approaches and LPs. It can be verified that the proposed method reduces the generation costs for all LPs when compared with all other presented approaches.

Also, Tables 1 and 2 show another interesting point. Comparing the case optimally operated with CHP plants with the one without CHP units (decoupled mode or conventional operation) for the suggested method indicates that for LP 1, 2, 3, and 4, gas production is increased by 42.31, 53.44, 38.91, and 31.26%, while the electrical generation is reduced by 54.29, 59.56, 44.63, and 72.66%, respectively; this is due to the fact that with CHP, the electrical power is

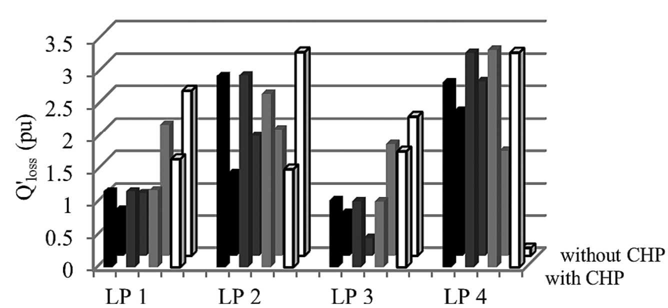

Fig. 9. Gas losses. Note: black, grey, dim-grey and white colors denote TVAC-PSO, PSO, GA, and DE, respectively.

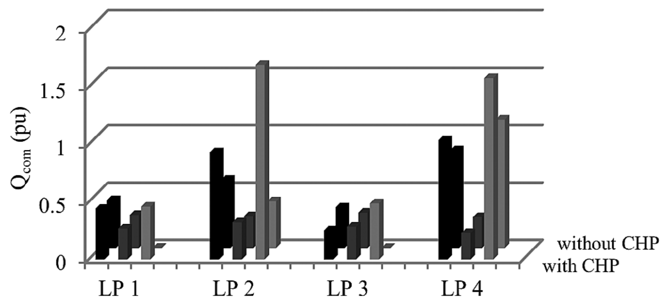

Fig. 10. Compressor demands. Note: black, grey, and dim-grey colors denote Q_{com_1}, Q_{com_2}, and Q_{com_3}, respectively.

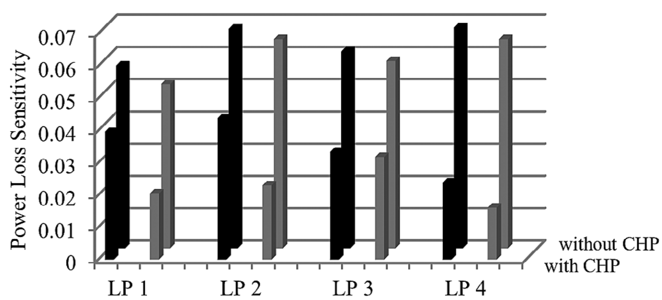

Fig. 11. Power loss sensitivities with respect to generator units. Note: black and dim-grey colors denote the power loss sensitivities with respect to G_1 and G_2, respectively.

locally generated and, as a result, the electrical productions of generators are reduced decreasing the electrical power transportation on long distances to load centers and consequently reducing the electrical losses.

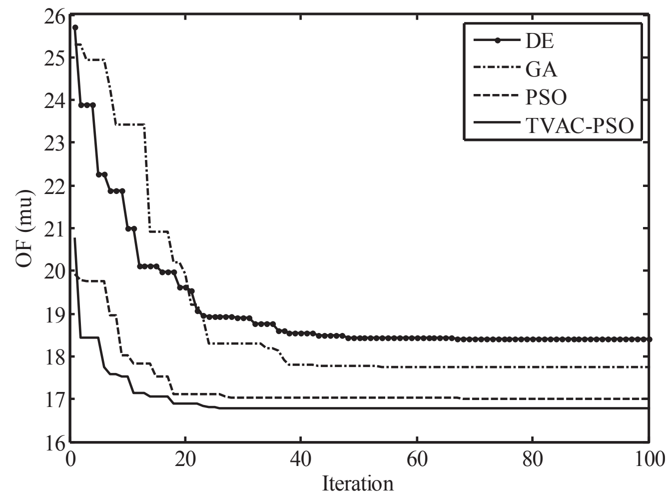

Fig. 13. Convergence curves of different methods for LP 1 with CHP.

The electrical and gas losses are shown in Figs. 8 and 9, respectively. Under this condition, in the case of connected CHP units compared with the case without CHP units for TVAC-PSO, electrical losses are reduced by 66.38, 74.09, 67.94, and 89.31%, while the gas losses are increased by 65.62, 130.67, 55.39, and 27.20% for LP 1, 2, 3, and 4, respectively. This result indicates that locally supplying electrical power through CHPs in the energy hubs has to be preferred. Fig. 10 illustrates consumption of each compressor for coupled (with CHPs) and decoupled (without CHPs) modes. Accordingly, in comparison with decoupled mode,

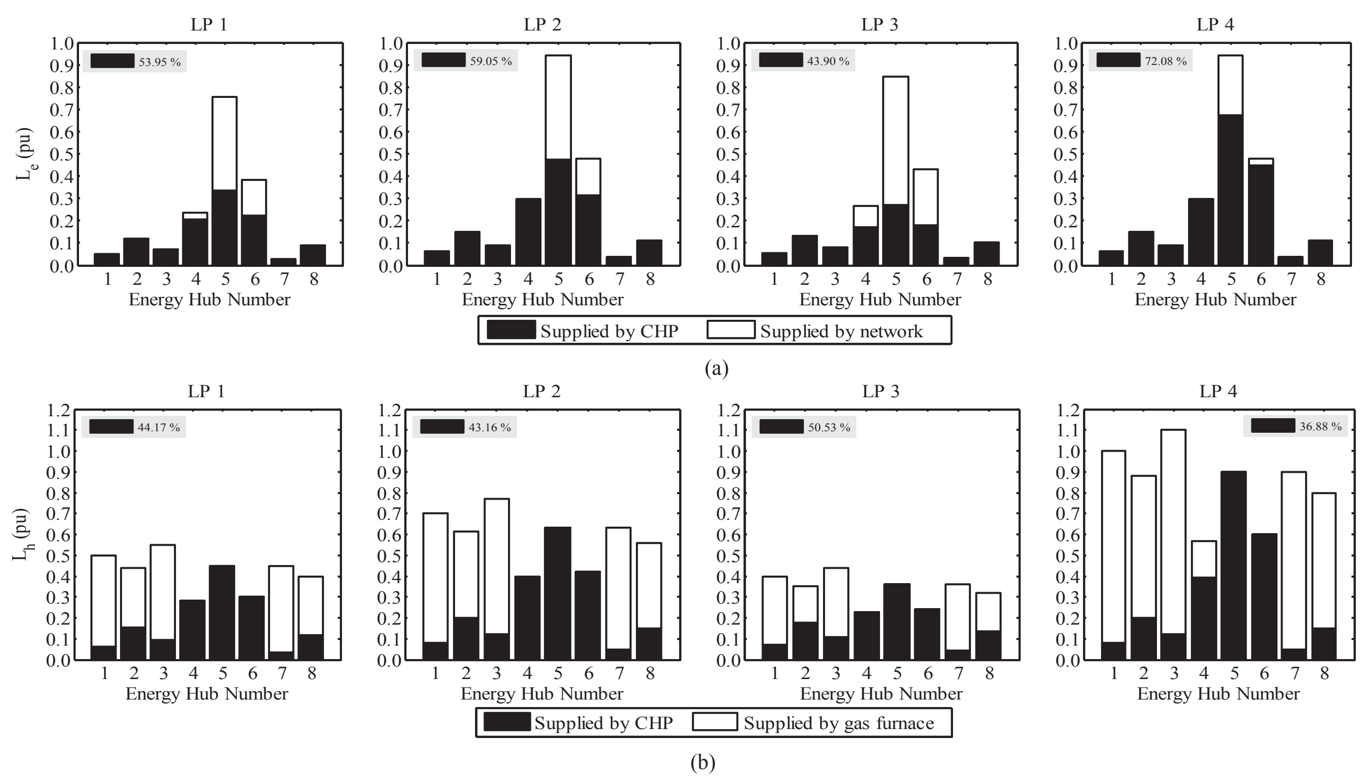

Fig. 12. Supplying the hub loads based on the TVAC-PSO (a) electrical demand of each hub (b) heat demand of each hub. Note: the percentages located at the top-left corner of each figure, shows the CHP contribution in supplying the hub demand. For example, Fig. 12(a) for LP 1emand is supplied through the CHP units and the rest of loads are provided by the electrical system.

Table 3
CPU times for different method for LP 1.

Technique	CPU Time [s]	
	With CHP	Without CHP
TVAC-PSO	8.1895	5.6668
PSO	8.9840	5.8289
GA	10.5523	6.3753
DE	11.0838	6.6353

the overall demands are increased (specially, the third compressor unit) to supply more gas into the pipeline system. This is due to the CHPs which locally produce more electricity as well as heat. As a result, the gas losses are increased in comparison with the conventional operation. Fig. 11 shows the power loss sensitivities with respect to generator units for two mentioned modes of operation. The power loss sensitivity illustrates an approximate change in the power losses due to the changes in the power generation. This figure indicates that the power loss sensitivity considering CHP units is reduced in comparison with another mode. This means that, in the coupled mode, generator units play a lesser role in changing the power losses (due to the CHPs). Moreover, the first generator plays a more prominent role than another.

Fig. 12 shows the hub demands for both electricity and heat. It can be observed that CHPs supply about 54, 59, 44, and 72% of the total real electrical demand L_e for the mentioned LPs (Fig. 12 (a)). Also, the second part of this figure (Fig. 12 (b)) shows that these devices can supply about 44, 32, 50, and 37% of the total heat demand for the same LPs. In other words, gas furnaces have a great role in supplying the heat demand L_h due to their higher efficiencies. In order to compare the convergence speed of different algorithms analyzed in this paper, LP 1 is selected for optimally utilization of CHPs. Fig. 13 shows the convergence curves of the TVAC-PSO, PSO, GA, and DE techniques in presence of CHPs. The suggested TVAC-PSO algorithm reaches a better solution than the other presented methods. The same conclusion has been observed for other LPs with and without using CHP units. Consequently, the convergence characteristic of the proposed approach is faster than the other reported techniques. Table 3 reflects the average CPU times for the studied algorithms based on LP 1. This table shows that the optimal operation with CHP units requires a higher CPU time compared with the conventional operation. This can be expected; because a greater number of variables must be treated. According to Tables 1–3, it is clear that the suggested approach provides better solutions with lower production costs and CPU times.

7. Conclusion

In this work, an optimization problem, namely MECED, was proposed and optimized through a suggested algorithm based on

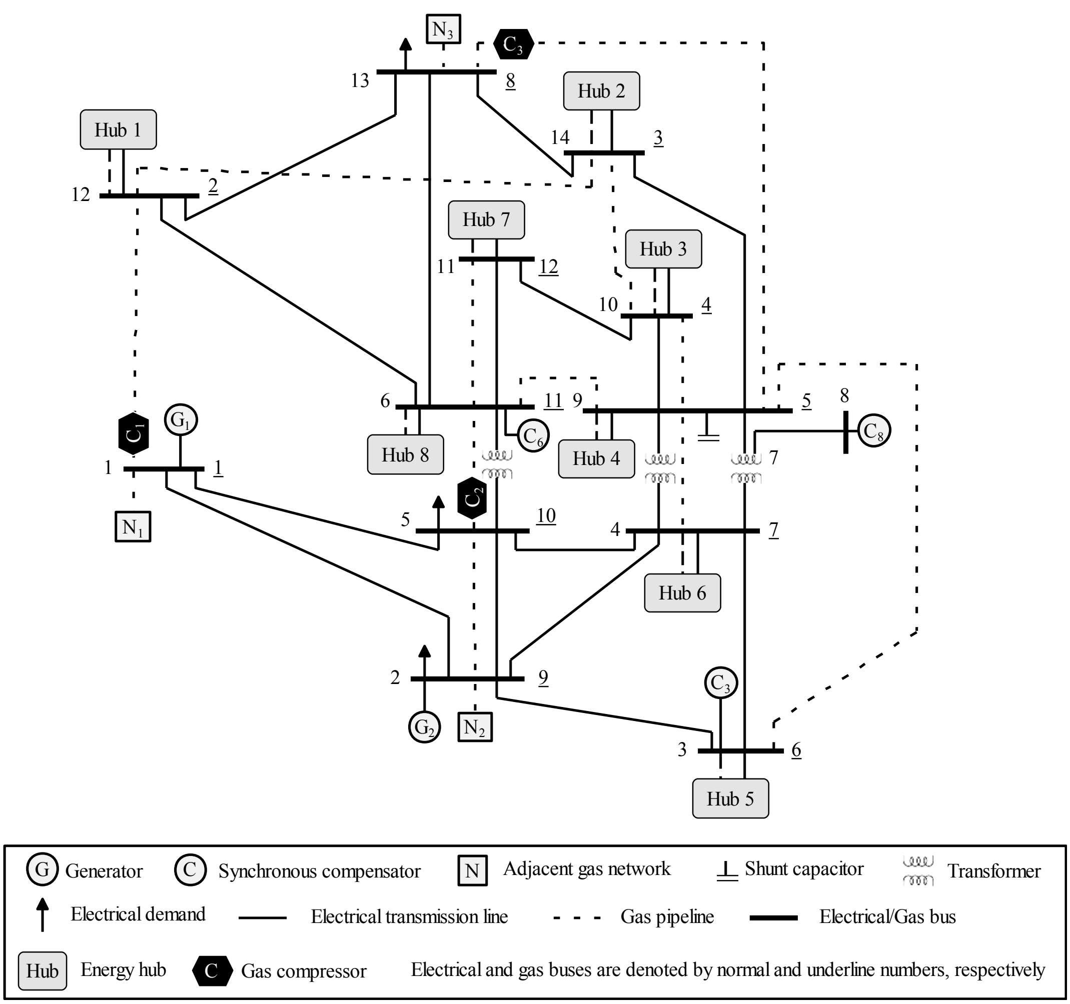

Fig. 14. The under study multi-carrier system.

the TVAC-PSO. The importance of this topic can be due to the need for an efficient use of energy, cost optimization in energy hubs, hybrid systems, integrated industrial districts, large tertiary facilities, etc. Hence, sum of the complexity of each energy system can significantly increase the computational burden. Important features associated with the problem formulation, which were addressed in this work, were the formulation of energy losses and the definition of economic dispatch in the hybrid system environments. The proposed approach was verified using two case study systems and numerical results reflected the following points: a) A hybrid system (gas-electric network) can operate at a lower cost than independently-operated systems. b) In the tested system, CHP supplied more electrical demand than the electrical network (except LP 3), while its contribution in supplying the heat demand was smaller than that of gas furnaces. This implies that in hybrid system, energy efficiency can be reached, producing electrical power and heat locally. c) CHP units in the energy hubs had a great role to reduce the operational cost. d) In the coupled mode (with CHP), electrical power losses were decreased, while the gas losses were increased. e) The proposed gas loss formula is simple to implement and could provide acceptable results. f) In order to reduce the absolute errors of the introduced gas loss formula, two adaptive values for compression ratios (ρ_{cr}) and dispatch factors (df) can be considered. g) For operating points far from the current one, it is suggested to update coefficients of gas loss formula to increase its accuracy. h) Cost reductions due to employing CHP units and applying the proposed optimization technique were greater than the other methods used for purpose of comparison in this paper. i) The suggested algorithm provided better quality solutions than those found by PSO, GA, and DE techniques.

Different energy systems considering their transmission capacities, various converters, formulation of various types of losses, electricity and gas storage modeling, different optimization techniques, and a more deep mathematical modeling of various elements are further model refinements to be considered in the future work on the subject.

Appendix

System data of test case B

A single-line diagram of the under study network is depicted in Fig. 14. The electrical system is based on the modified IEEE 14-bus network including generators G_1 and G_2 at buses 1 and 2, respectively; synchronous compensators C_3, C_6, and C_8 at bus 3, 6, and 8, respectively; 20 transmission lines; including two transformers at connections 5–6 and 4–7–9; and a single shunt capacitor at bus 9. The pipeline network (gas-based system) contains three gas sources at buses $\underline{1}$, $\underline{8}$, and $\underline{9}$ (adjacent networks), three compressors at connections $\underline{1}$–$\underline{2}$, $\underline{10}$–$\underline{11}$, and $\underline{8}$–$\underline{5}$; and 11 pipelines. Also, there are 8 energy hubs which consume electricity as well as gas to supply electrical and heat loads. Hubs 1–8 are installed at buses 12, 14, 10, 9, 3, 4, 11, and 6 (or $\underline{2}$, $\underline{3}$, $\underline{4}$, $\underline{5}$, $\underline{6}$, $\underline{7}$, $\underline{12}$, and $\underline{11}$), respectively. It should be mentioned that Fig. 1 shows the structure of each energy hub in this system. The data of sources is as: N_1:slack, $ag_1 = 0$ mu, $bg_1 = 0.76$ mu/pu, $cg_1 = 0.03$ mu/pu^2, and $\rho_{\underline{1}} = 1.2$ pu; N_2:$ag_2 = 0$ mu, $bg_2 = 0.9$ mu/pu, $cg_2 = 0.04$ mu/pu^2, and $\rho_{\underline{9}} = 1.1$ pu; N_3:$ag_3 = 0$ mu, $bg_3 = 0.8$ mu/pu, $cg_3 = 0.02$ mu/pu^2, and $\rho_{\underline{8}} = 1.2$ pu; G_1:slack, $ae_1 = 0$ mu, $be_1 = 9.9$ mu/pu, $ce_1 = 0.0088$ mu/pu^2, and $0 \le AP_1^g \le 2.5$ pu; G_2:$ae_2 = 0$ mu, $be_2 = 10$ mu/pu, $ce_2 = 0.0045$ mu/pu^2, and $0 \le AP_2^g \le 2.5$ pu. Other data can be found in Ref. [20]. Note that, in this paper, the electrical system with two generators is considered.

References

[1] Mc Calley J, Krishnan V, Gkritza K, Brown R, Mejia-Giraldo D. Planning for the long haul: investment strategies for national energy and transportation infrastructures. IEEE Power Energy Mag 2013;11:24–35.

[2] Kieffer M, Brown T, Brown RC. Flex fuel polygeneration: integrating renewable natural gas into fischer–tropsch synthesis. Appl Energy 2016;170:208–18.

[3] Chiang N-Y, Zavala VM. Large-scale optimal control of interconnected natural gas and electrical transmission systems. Appl Energy 2016;168:226–35.

[4] Götz M, Lefebvre J, Mörs F, McDaniel Koch A, Graf F, Bajohr S, et al. Renewable power-to-gas: a technological and economic review. Renew Energy 2016;85:1371–90.

[5] Bensmann B, Hanke-Rauschenbach R, Müller-Syring G, Henel M, Sundmacher K. Optimal configuration and pressure levels of electrolyzer plants in context of power-to-gas applications. Appl Energy 2016;167:107–24.

[6] Geidl M, Koeppel G, Favre-Perrod P, Klockl B, Andersson G, Frohlich K. Energy hubs for the future. IEEE Power Energy Mag 2007;5:24–30.

[7] Ríos-Mercado RZ, Borraz-Sánchez C. Optimization problems in natural gas transportation systems: a state-of-the-art review. Appl Energy 2015;147:536–55.

[8] Vesterlund M, Dahl J. A method for the simulation and optimization of district heating systems with meshed networks. Energy Convers Manag 2015;89:555–67.

[9] Geidl M, Andersson G. Optimal power flow of multiple energy carriers. IEEE Trans Power Syst 2007;22:145–55.

[10] Shabanpour-Haghighi A, Seifi AR. Energy flow optimization in multicarrier systems. IEEE Trans Ind Inf 2015;11:1067–77.

[11] Moeini-Aghtaie M, Abbaspour A, Fotuhi-Firuzabad M, Hajipour E. A decomposed solution to multiple-energy carriers optimal power flow. IEEE Trans Power Syst 2014;29:707–16.

[12] REAPower n.d. http://www.reapower.eu/project-scope (Accessed 5 March 2017).

[13] Energy hub management system project n.d. https://uwaterloo.ca/energy-hub-management-system/(Accessed 5 March 2017).

[14] An S, Li Q, Gedra TW. Natural gas and electricity optimal power flow. In: IEEE PES Transm. Distrib. Conf. Expo., Dallas, TX; 2003. p. 138–43.

[15] Geidl M, Andersson G. Optimal power dispatch and conversion in systems with multiple energy carriers. In: 15th Power Syst. Comput. Conf., Liège, Belgium; 2005.

[16] Majidi M, Nojavan S, Zare K. A cost-emission framework for hub energy system under demand response program. Energy 2017;134:157–66.

[17] Derafshi Beigvand S, Abdi H, La Scala M. A general model for energy hub economic dispatch. Appl Energy 2017;190:1090–111.

[18] Dolatabadi A, Mohammadi-Ivatloo B. Stochastic risk-constrained scheduling of smart energy hub in the presence of wind power and demand response. Appl Therm Eng 2017;123:40–9.

[19] Vahid-Pakdel MJ, Nojavan S, Mohammadi-ivatloo B, Zare K. Stochastic optimization of energy hub operation with consideration of thermal energy market and demand response. Energy Convers Manag 2017;145:117–28.

[20] Derafshi Beigvand S, Abdi H, La Scala M. Optimal operation of multicarrier energy systems using time varying acceleration coefficient gravitational search algorithm. Energy 2016;114:253–65.

[21] Derafshi Beigvand S, Abdi H, La Scala M. Multicarrier energy system optimal power flow. From smart grids to smart cities new challenges Optim. energy grids. John Wiley & Sons; 2017. p. 273–303.

[22] Shao C, Wang X, Shahidehpour M, Wang X, Wang B. An MILP-based optimal power flow in multicarrier energy systems. IEEE Trans Sustain Energy 2017;8:239–48.

[23] Mahor A, Prasad V, Rangnekar S. Economic dispatch using particle swarm optimization: a review. Renew Sustain Energy Rev 2009;13:2134–41.

[24] AlRashidi MR, El-Hawary ME. A survey of particle swarm optimization applications in electric power systems. IEEE Trans Evol Comput 2009;13:913–8.

[25] Basu M. Modified particle swarm optimization for nonconvex economic dispatch problems. Int J Electr Power Energy Syst 2015;69:304–12.

[26] Ghasemi M, Aghaei J, Akbari E, Ghavidel S, Li L. A differential evolution particle swarm optimizer for various types of multi-area economic dispatch problems. Energy 2016;107:182–95.

[27] Pratap Singh R, Mukherjee V, Ghoshal SP. Particle swarm optimization with an aging leader and challengers algorithm for optimal power flow problem with FACTS devices. Int J Electr Power Energy Syst 2015;64:1185–96.

[28] Derafshi Beigvand S, Abdi H, La Scala M. Hybrid gravitational search algorithm-particle swarm optimization with time varying acceleration coefficients for large scale CHPED problem. Energy 2017;126:841–53.

[29] Mohammadi-Ivatloo B, Moradi-Dalvand M, Rabiee A. Combined heat and power economic dispatch problem solution using particle swarm optimization with time varying acceleration coefficients. Electr Power Syst Res 2013;95:9–18.

[30] Chaturvedi KT, Pandit M, Srivastava L. Particle swarm optimization with time varying acceleration coefficients for non-convex economic power dispatch. Int J Electr Power Energy Syst 2009;31:249–57.

[31] Geidl M. A greenfield approach for future power systems. Paris, France: Cigre

Sess. 41; 2006.
[32] Frik R, Favre-Perrod P. Proposal for a multifunctional energy bus and its interlink with generation and consumption. 2004.
[33] Binetti G, Davoudi A, Naso D, Turchiano B, Lewis FL. A distributed auction-based algorithm for the nonconvex economic dispatch problem. IEEE Trans Ind Inf 2014;10:1124–32.
[34] Sun J, Palade V, Wu X-J, Fang W, Wang Z. Solving the power economic dispatch problem with generator constraints by random drift particle swarm optimization. IEEE Trans Ind Inf 2014;10:222–32.
[35] Geidl M. Integrated modeling and optimization of multi-carrier energy systems. 2007. ETH Zurich.
[36] Geidl M, Andersson G. A modeling and optimization approach for multiple energy carrier power flow. St. Petersburg, Russian Federation: IEEE Russ. Power Tech; 2005. p. 1–7.
[37] Saadat H. Power system analysis. PSA Publishing LLC; 2011.
[38] Vasconcelos CD, Lourenço SR, Gracias AC, Cassiano DA. Network flows modeling applied to the natural gas pipeline in Brazil. J Nat Gas Sci Eng 2013;14:211–24.
[39] Shanbi P, Junying L, Yong J, Yuan L. The simulation of natural gas gathering pipeline network. Open Fuels Energy Sci J 2013;6:18–22.
[40] Debebe A, Majid A, Amin M. Simulation of natural gas transmission pipeline network system performance. J Energy Power Eng 2009;3:19–30.
[41] Kennedy J, Eberhart R. Particle swarm optimization. In: Proc. IEEE Int. Conf. Neural networks, Perth, WA; 1995. p. 1942–8. p.
[42] Clerc M, Kennedy J. The particle swarm – explosion, stability, and convergence in a multidimensional complex space. IEEE Trans Evol Comput 2002;6: 58–73.